Lattice dynamics and superconducting T_c for dilute H and D interstitials in Al

D. W. Taylor
Physics Department, McMaster University, Ontario, Canada
(Received 18 December 1979)

The lattice dynamics of isolated H and D interstitial ions in Al have been calculated with the initial aim of establishing the local mode frequencies. Kohn-Sham nonlinear screening was used for the H,D potentials, anharmonic effects due to the large interstitial motion were accounted for within a quasiharmonic approximation, and the relaxations of the Al neighbors of an interstitial were also included. The calculations were carried out for both the octahedral and tetrahedral interstitial sites, and they predict a local mode frequency well separated from the Al phonon frequency, with the possible exception of octahedral D. Small, but not negligible, anharmonic effects are predicted. These show up very strongly in the calculation of the changes in T_c due to low concentrations of interstitials ($\leq 1\%$). A definite inverse isotope effect is predicted if it is the octahedral site that is occupied, whereas only a very weak isotope effect is predicted for the tetrahedral case.

I. INTRODUCTION

The introduction of large quantities of interstitial H and D into Al films, via ion implantation, produces dramatic increases in the superconducting transition temperature, T_c.[1,2] An H concentration in the region of 200 at.% (i.e., AlH_2) produces an increase in T_c from 1.18 to 6.75 K,[1] whereas 30 at.% H produces a T_c of 5.95 K with 30 at.% D giving 5.7 K.[2] However superconducting tunneling into such films has not yet yielded any evidence of a high-frequency impurity band due to either H or D.[2] Instead the presence of the interstitials enhances the longitudinal phonon peak in the tunneling characteristics. Kus and Carbotte[3] have shown that this could be due to a high-frequency contribution to $\alpha^2 f(\omega)$, although the possibility of a resonance around the Al longitudinal peak could not be ruled out.

This suggests a theoretical investigation of whether a high-frequency peak should be expected. A first step, which is taken here, is to calculate the effect of a low concentration of interstitials. This is motivated by the assumption that the frequency of any predicted local mode indicates the approximate position of an impurity band formed at much larger concentrations. This neglects the possibility of significant contributions from the long-range interactions between the interstitials and from any volume change due to the presence of the interstitials.

Calculations for this system are simpler than those for the highly investigated transition metal-H systems[4] in that a simple pseudopotential can be used for the host crystal potential and band-structure effects are not so important. This relative simplicity means that we have been able to make predictions about the effects due to the introduction of the interstitials using only experimental information about the host material. The evaluation of the phonon Green's functions required the Al phonon dispersion curves and this same information was also used to determine the parameters in the Al pseudopotential. The potential for the interstitial ion was taken from calculations[5] that used a Kohn-Sham nonlinear screening approximation.[6] The resulting interstitial-Al potential could then be used to calculate the interstitial-Al force constants using a self-consistent quasiharmonic approximation[7] to allow for anharmonic effects. This is to be contrasted with the simplified anharmonic perturbation theory so far used for Pd-H,D.[8] Having such a potential we were also able to investigate the consequences of the relaxation of the Al neighbors of an interstitial ion.

We have calculated the dynamics of the Al-H,D system with the Al ions assumed static and free to move. As we also wished to calculate the effects of the interstitials on the electron-phonon function $\alpha^2 f(\omega)$ we have used a procedure that does not eliminate the host-lattice sites.[9] This contrasts with the method used by Lottner *et al.*[10] to describe the motion of H in Nb, V, and Ta. Section II of this paper describes the theory used for the interstitial dynamics as well as for the anharmonic corrections and relaxation. The numerical results are discussed in some detail in Sec. III.

One interesting feature of the Pd-H,D system is the occurrence of an inverse isotope effect for T_c. This is thought to be anharmonic in origin, either directly via the lattice dynamics as proposed by Ganguly[11] or indirectly through modifications to the electronic structure.[12] To this end we have investigated the effects of low concentrations of H or D on the value of T_c using the results of the dynamical cal-

culations described in this paper. The approximate weak-coupling theory for T_c which includes the effect of the washing out of electron-phonon anisotropy is described in Sec. IV A along with the details of the calculation of $\alpha^2 f(\omega)$. The numerical results are analyzed in Sec. IV B where we see that, indeed, our results do predict a significant isotope effect for octahedral interstitials.

The question as to which kind of interstitial site is occupied by H and D ions has not yet been fully answered. Early theoretical calculations[5] indicate that it is the octahedral site that is occupied. However, a very recent calculation by Larsen and Norskov[13] favors the tetrahedral site. Channeling experiments[14] indicate that the interstitials are at tetrahedral sites, possibly associated with a vacancy. However, the interstitial concentrations were not indicated. The tunneling results[1] that claim a 200 at.% interstitial concentration also indicate, that at least at large concentrations, the occupied site is the tetrahedral one. Being originally based on the earlier calculations this paper gives more details for the octahedral site but all the calculations have been done for both.

II. THEORY FOR LATTICE DYNAMICS

A. Interstitial-aluminum potential

The inclusion of a proton within an electron gas produces large changes in the electron density that linear screening approximations do not describe in a reliable manner. A suitable nonlinear theory for calculating these changes is that of Kohn and Sham.[6] With this density functional theory it should be possible to calculate directly an ion-ion interaction of the kind required here. However such a calculation would be rather complicated with the ion-ion separation entering both the kinetic- and potential-energy terms.[15] Further, such a calculation would require a similar treatment of the charge cloud around the aluminum core. Such calculations are only just becoming available.[16]

Instead we have resorted to the pseudopotential result

$$V(R) = -Z/R + U(R) \ , \tag{1}$$

where Z is the charge on the aluminum ion and $U(R)$ is electron-ion contribution

$$U(R) = \int n(\vec{R}-\vec{r})\, w(\vec{r})\, d^3r = \frac{1}{(2\pi)^3}\int n(q)\, w_{\mathrm{Al}}(q)\, e^{i\vec{q}\cdot\vec{R}}\, dq \ . \tag{2}$$

However instead of using linear screening to calculate the electron density $n(\vec{r})$ around the interstitial ion, we have used the results of the nonlinear theory referred to above. For the Al pseudopotential, $w_{\mathrm{Al}}(r)$, we have used a local form of the Heine-Abarenkov potential

$$w_{\mathrm{Al}}(r) = \begin{cases} -ZA/R_m \ , & r < R_m \ , \\ -Z/R \ , & r > R_m \ . \end{cases} \tag{3}$$

B. Self-consistent harmonic approximation

The large vibrational motion expected of the light interstitial ions indicates that the above potential should not be used to construct just a harmonic Hamiltonian for the system. Instead anharmonic effects should be taken into account. To do this we have used a renormalized harmonic Hamiltonian[17] following the prescription of Gillis *et al.*[7] Thus the potential $V(\vec{R}(l)-\vec{R}(l'))$, between an interstitial and an aluminum ion whose equilibrium positions are at $\vec{R}(l)$ and $\vec{R}(l')$, is replaced by

$$\langle V(\vec{R}(l,l')+\vec{u}(l)-\vec{u}(l'))\rangle = [(2\pi)^3 \det \underline{D}(l,l')]^{-1/2}\int d^3u\, V(\vec{R}(l,l'+\vec{u}))\exp\left(-\frac{\vec{u}\cdot\underline{D}(l,l')^{-1}\cdot\vec{u}}{2}\right) \ . \tag{4}$$

The matrix $\underline{D}(l,l')$ is the thermal average

$$D_{\alpha\beta}(l,l') = \langle [u_\alpha(l)-u_\alpha(l')][u_\beta(l)-u_\beta(l')]\rangle_T \tag{5}$$

calculated in the harmonic approximation and $\vec{u}(l)$ is the displacement from equilibrium.

As the interstitial motion can be expected to dominate $\underline{D}(l,l')$, and this motion should be isotropic, we have simplified our calculations by replacing $\underline{D}(l,l')$ by its isotropic average $\bar{D}$. If $\vec{R}(l,l')$ is taken to be along Ox then

$$D_{\alpha\beta}(l,l') = \bar{D}(l,l')\delta_{\alpha\beta}$$

with

$$\bar{D}(l,l') = \tfrac{1}{3}[D_{xx}(l,l')+2D_{yy}(l,l')] \ . \tag{6}$$

Our numerical results indicate that D_{xx} and D_{yy} differ by less than 20% with the major difference coming from the correlation functions for displacements on different sites. Hence we can now write

$$\langle V(\vec{R}(l,l')+\vec{u}(l)-\vec{u}(l'))\rangle = [2\pi\bar{D}(l,l')]^{-3/2}\int d^3u\, V(\vec{R}(l,l')+\vec{u})\, e^{-u^2/2\bar{D}(l,l')} = \int d^3q\, V(q)\, e^{-\bar{D}(l,l')q^2/2} e^{i\vec{q}\cdot\vec{R}(l,l')} \ . \tag{7}$$

In our calculations the average of the Coulomb term was calculated in real space and the electron-ion term $U(R)$, in $\vec{q}$ space.

C. Relaxation

The inclusion of interstitial ions within the Al lattice can be expected to cause changes in the equilibrium positions of the neighboring Al ions. We have calculated the values for these relaxations using the method of lattice statics.[18] This requires that the potential energy of the lattice be minimized with respect to the relaxations $\vec{\Delta}(l)$ from the pure Al positions, $\vec{R}^0(l)$.

Hence if the lattice potential energy is

$$\langle V\rangle = \frac{1}{2}\sum_{l\neq l'}\langle V(\vec{R}(l,l')+\vec{u}(l)-\vec{u}(l'))\rangle \tag{8}$$

with

$$\vec{R}(l,l') = \vec{R}^0(l)+\vec{\Delta}(l)-\vec{R}^0(l')-\vec{\Delta}(l')$$

then we must set

$$d\langle V\rangle/d\Delta_\alpha(l) = 0$$

to give

$$\left\langle \frac{\partial}{\partial\Delta_\alpha(l)} V(\vec{R}^0(l,i)+\vec{\Delta}(l))\right\rangle + \sum_{\beta l'}\langle\Phi_{\alpha\beta}(ll')\rangle\Delta_\beta(l') = 0 \tag{9}$$

The interstitial ion has been taken to be at $\vec{R}(i)$. The renormalized force-constant matrix should be evaluated at the relaxed positions. This requires the iteration of Eq. (9). The matrix manipulations required by this method follow naturally from those required in the dynamical calculations (see next section).

D. Lattice dynamics

With the determination of the force constants between the interstitial ion and the Al ions at their relaxed positions, the calculation of the dynamics is a straightforward procedure.

1. Static lattice approximation

An estimate of the local mode frequency of an interstitial ion can be obtained by neglecting the motion of the Al host lattice. Due to the cubic symmetry of the crystal the Coulomb term in Eq. (1) makes no contribution to this frequency.

The local mode angular frequency ω_L for an interstitial ion at $\vec{R}(i)$ is then given by

$$\omega_L^2 = \frac{1}{M_i}\sum_l \frac{\partial^2}{\partial x^2} U(\vec{R}(i,l))$$

$$= -\frac{1}{6M_i\pi^2}\sum_n \frac{N_n}{R_n}\int dq q^3 \sin qR_n\langle U(q)\rangle \ , \tag{10}$$

where R_n is the distance of the nth shell of the Al ions from the interstitial ion, there being N_n ions in the shell. A convenient check on the convergence of this real-space sum is given by converting to reciprocal space. Then

$$\omega_L^2 = -\frac{1}{3M_i\Omega_0}\sum_n H_n^2\langle U(H_n)\rangle e^{i\vec{H}_n\cdot\vec{R}(i)} \ , \tag{11}$$

where the $\vec{H}_n$ are reciprocal lattice vectors and Ω_0 is the volume per Al ion.

The scheme for determining the potential used in Eqs. (10) and (11) is completed by using the zero-temperature result

$$\bar{D} = \langle u_x^2(i)\rangle = \frac{\hbar}{2M_i\omega_L} \ . \tag{12}$$

With an initial guess for ω_L we are in a position to iterate Eq. (7), (9), (10), or (11) through to convergence.

2. Dilute t-matrix approximation

The more elaborate procedure that allows for the motion of the host lattice has been long established.[9] Hence, we will give just a summary of the main results.

The displacement-displacement correlation $\langle u_\alpha(l)u_\beta(l')\rangle$ can be written in terms of the displacement-displacement Green's function, $G_{\alpha\beta}(ll';\omega)$

$$\langle u_\alpha(l)u_\beta(l')\rangle = \frac{\hbar}{\pi}\int_0^\infty \coth\left(\frac{\beta\omega}{2}\right)\mathrm{Im}G_{\alpha\beta}(l,l';\omega)\,d\omega \ . \tag{13}$$

It is the imaginary part of the Green's function evaluated just below the real axis that is used in Eq. (13). As we are only interested in the correlation function at very low temperatures the coth function can be replaced by unity as $\beta=\hbar/k_BT\to\infty$.

The Green's function $\underline{G}$ for the real system of the interstitial ions coupled to the host ions, is related to that for the so-called unperturbed system of the interstitial ions uncoupled from the host ions $\underline{P}$ via the equation

$$\underline{G} = \underline{P}+\underline{P}\,\underline{C}\,\underline{G} \ , \tag{14}$$

where $\underline{C}$ contains the changes in the force constants due to presence of the interestitial ions. Here

$$P_{\alpha\beta}(l,l';\omega) = \frac{1}{NM}\sum_{j\vec{q}}\sigma_\alpha^j(\vec{q})\sigma_\beta^j(\vec{q})e^{i\vec{q}\cdot\vec{R}^0(l,l')}P_j(\vec{q},\omega) \ , \tag{15}$$

$$P_j(\vec{q},\omega) = [\omega^2-\omega_j^2(\vec{q})]^{-1} \ ,$$

is the Green's function for the unperturbed Al crystal which has N ions of mass M at sites $\vec{R}^0(l)$. $\omega_j(\vec{q})$

and $\vec{\sigma}_j(\vec{q})$ are the eigenvalue and eigenvector of the phonon mode j of wave vector $\vec{q}$. The unperturbed Green's function for an interstitial ion of mass M_i at $\vec{R}_i$ is

$$P_{\alpha\beta}(ii) = (1/M_i\omega^2)\delta_{\alpha\beta} \ . \tag{16}$$

In the dilute limit, when the defect spaces of individual interstitial ions do not overlap, the matrix $\underline{C}$ can be written as

$$C_{\alpha\beta}(l,l') = \sum_i C^i_{\alpha\beta}(l,l') = \sum_i \langle \Phi^i_{\alpha\beta}(l_i l_i') \rangle \ , \tag{17}$$

where l_i, l_i' are confined to the defect space of the ith interstitial ion. The Φ^i couple just the interstitial and host atoms, and no changes in the force constants between the host ions were taken into account.

For very low concentrations of interstitial ions a satisfactory solution to Eq. (14) that is suitable for our purposes is[9]

$$\underline{G} = \underline{P} + \underline{P} \sum_i \underline{T}^i \underline{P} \ , \tag{18}$$

where the t matrix for ith interstitial is

$$\underline{T}^i = \underline{C}^i (1 - \underline{P}\underline{C}^i)^{-1} \ . \tag{19}$$

To obtain the displacement-displacement correlated functions needed to calculate the self-consistent harmonic potential, Eq. (18) was itself simplified further by including just one interstitial in the crystal.

In order to invert the matrix in Eq. (19) it is necessary to transform to the irreducible representations of the symmetry group of the defect space. This was done by using the transformation matrices[19] ψ via

$$\sum_{\alpha\beta, l_i l_i'} \psi^{s a \lambda}(l_i) C^i_{\alpha\beta}(l_i, l_i') \psi^{s b \lambda}_{\beta}(l_i') = C^s_{ab} \ . \tag{20}$$

Here λ labels the row of sth representation which may appear more than once (label a). Using the tables given by Maradudin[20] the ψ matrices can be readily formed for the cases of interest here.

(i) For an interstitial at an octahedral site, $(\frac{1}{2}a, \frac{1}{2}a, \frac{1}{2}a)$, in an fcc lattice ($a$ being the lattice constant) the nearest Al neighbors are located on a simple cubic (sc) lattice and the next-nearest neighbors are on a bcc lattice. Hence if just nearest neighbors are taken into account, the matrices in the defect space reduce according to

$$A_{1g} + E_{1g} + T_{1g} + T_{2g} + 3T_{1u} + T_{2u} \ .$$

Including the next-nearest neighbors gives

$$2A_{1g} + 2E_g + 2T_{1g} + 3T_{2g} + A_{2u} + E_u + 5T_u + 2T_{2u} \ .$$

(ii) For an interstitial atom at a tetrahedral site, $(\frac{1}{4}a, \frac{1}{4}a, \frac{1}{4}a)$ taking into account just the nearest neighbor gives

$$A_1 + E + T_1 + 3T_2 \ .$$

The local mode frequencies are found by looking for zeros in the denominators of the T matrices of the different irreducible representations.

This use of symmetry also simplifies the relaxation calculation for the relaxation of ions that are within the defect space. The forces producing the relaxation $\langle \vec{\nabla} V \rangle$ are all radial so only the A_{1g} or A_g representation is needed. Further, the full-force-constant matrix $\langle \Phi \rangle$ is given by the zero-frequency limit of $-G^{-1}$ in the one interstitial limit. Hence Eq. (9) has the form

$$\Delta^s_a = \sum_b G^s_{ab} \langle \vec{\nabla} V \rangle^s_b \tag{21}$$

with $s \equiv A_{1g}$ or A_g as appropriate.

Hence we have a complete scheme of proceeding from an initial guess for $\bar{D}$ to calculate $\langle V \rangle$, then to the relaxations and the $\langle \Phi \rangle$'s and finally via the Green's functions to the displacement correlation functions and $\bar{D}$.

III. RESULTS FOR THE INTERSTITIAL DYNAMICS

We must first describe our input data. As it was readily available we used the tabulated $n(r)$ as calculated by Popović *et al.*[5] for a unit charge in an electron gas of density appropriate to that of Al. Although improved solutions of the Kohn-Sham theory have been described,[21] they result in very small changes in $n(r)$ at the values of r that are of interest here. The parameters for the Al pseudopotential were taken from a fit, due to Brovman and Kagan,[22] to the measured phonon dispersion curves. Their fit corresponds to $R_m = 1.213\, a_0, A = 0.182$. The Al Green's functions were calculated in the usual manner by first calculating the imaginary parts and then using a Hilbert transform to obtain the real parts. The sums over $\vec{k}$ were handled using the methods of Gilat and Raubenheimer[23] and Al phonon eigenvalues and eigenvectors were calculated using the Born–von-Karman fit to the 80-K experimental phonon dispersion curves due to Gilat and Nicklow.[24]

A. Static lattice

Although the relaxation of the Al ions around the interstitial ion can be readily incorporated in the static-lattice approximation (SLA), the calculation of the relaxation itself is not such a simple calculation. Further, we used this approximation largely to investigate the question of the range of the force constants. Hence, relaxation was neglected in the self-consistent SLA.

Our results for the interstitial frequencies are presented in Table I. In this table $\nu_L^{(1)}$ and $\nu_L^{(2)}$ are the values for the local mode frequencies obtained by

TABLE I. Local mode frequency in the static-lattice approximation.

	Interstitial ion	$\bar{D}^{1/2}$ (Å)	$\nu_L^{(1)}$	$\nu_L^{(2)}$ (THz)	ν_L
Octahedral	D	0.144	9.83	10.49	12.07
	H	0.165	15.70	16.58	18.38
Tetrahedral	D	0.099	24.59	26.24	25.77
	H	0.117	35.35	37.64	36.89

summing in Eq. (10) just as far as the first- and second-nearest neighbors, respectively. For the octahedral interstitial, it can be seen that including just nearest-neighbor (NN) forces gives a local mode frequency that is 15–20% too low and even including the forces from the next-nearest neighbors (NNN), the frequency is still about 10% too low. To further illustrate the effect of distant neighbors we plot ν_L for D, as a function of the neighbor distance in Fig. 1. The number of neighbors at a given distance is indicated by the vertical lines. It is only by the 7th NN that a good value of ν_L is obtained. The value of ν_L, as obtained from Eq. (11) by summing in reciprocal space, is also shown on the diagram, and the real-space values of ν_L converge quite well to this value. The contribution to ν_L due to the distant neighbors is much smaller for the tetrahedral interstitial. Even just the NN forces give a value for ν_L that is only 5% too low. A graph similar to Fig. 1 shows that after an overshoot due to the NNN forces, the value of ν_L drifts slowly down, albeit with some noise, towards the correct value, and is in very good agreement by the 5th NN. This behavior must be due to the fact that in the tetrahedral case the very strong NN forces dominate over all the others.

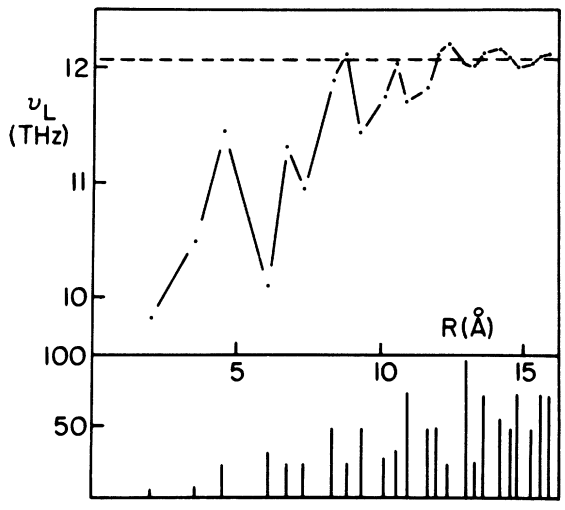

FIG. 1. The static-lattice approximation for the local mode frequency ν_L, for an octahedral interstitial D ion as a function of the number of shells of neighbors included in the sum in Eq. (10). R is the radius of a shell and the dashed line is the result of Eq. (11). The lower bar graph gives the number of Al ions in each shell.

These large values of ν_L, particularly for the tetrahedral interstitial, give some support to the conjecture of Kus and Carbotte[3] that there exists a high-frequency mode in concentrated Al-H,D.

The self-consistent values of $\bar{D}$ quoted in Table I indicate values for the root mean-square displacement of the interstitial that are about 10% of the NN distances (tetrahedral, 1.75 Å; octahedral, 2.02 Å). Hence appreciable anharmonic effects are to be expected. For instance, corrections can be expected to the ratio

$$R_L = M_H \nu_L^2(H)/M_D \nu_L^2(D) \ ,$$

which should equal one in the harmonic approximation. In the octahedral case this is, indeed, the case as the results in Table I give $R_L = 1.16$. However for the tetrahedral case the much larger values of ν_L, and hence the smaller values of $\bar{D}$, result in smaller anharmonic corrections and the ratio R_L drops to 1.03. The result for the octahedral case is reminiscent of the experimental value found for Pd-H,D where $R_L = 1.2$.[25] This enhancement is thought to be the major contribution to the inverse isotope effect in this Pd system.[11,26] The very small enhancement of R_L for the tetrahedral site is at least a change in the right direction from the octahedral result as experiments on concentrated Al-H,D alloys[2] show a normal isotope effect.

In closing we note that the presence of the exponential falloff in Eq. (7) due to the anharmonic renormalization has a calculational benefit in that ν_L is insensitive to values of $n(q)$ for q beyond $10\,a_0^{-1}$. In the absence of the renormalization we found that in

order to get convergence of both Eqs. (10) and (11) it was necessary to go to much larger values of q. This necessitated modeling $n(q)$ using a Thomas-Fermi form for $q > 15a_0^{-1}$ due to shortcomings in the tabulated $n(q)$. Happily, this was not called for in the work reported here.

B. Dynamic lattice

The significant effect on ν_L due to distant neighbors, found in the SLA, poses a difficulty for the much more lengthy dynamical calculations. It would take a lot of work to extend the analysis of Sec. II D beyond the second NN's of the octahedral interstitial and it does not seem worth doing, as the required computational time would become very expensive. Instead we resorted to a scaling procedure.

For the octahedral case we used the SLA to determine a scaling factor α for the NNN force constants. This was done by requiring that $\nu_L^{(2)}$, calculated using the scaled NNN force constants and the unscaled NN force constants, agreed with ν_L (all calculated using the SLA approximation). As the effect of the distant neighbors is not so important in the tetrahedral case we merely scaled the NN forces such that $\nu_L^{(1)}$ agreed with ν_L.

The results of our calculations are given in Tables II and III for the octahedral and tetrahedral interstitials, respectively. The force constants quoted are those longitudinal and transverse to the bond and include the scaling introduced above. We note that the renormalization equation (7) calls for different $\bar{D}$ depending upon which bond the force constants are being calculated. However, as our numerical results indicated that the $\bar{D}$ for the NN and NNN bonds of an octahedral interstitial differ by no more than 5%, the same (NN) $\bar{D}$ was used for both bonds.

In Table III, two local mode frequencies are quoted. The lower one refers to a local mode of A_1 symmetry and so is not directly dependent on the interstitial mass. It is also quite weak. The other value of ν_L corresponds to the expected mode of T_2 symmetry. The octahedral local mode referred to in Table II has T_{1u} symmetry.

The initial line in these tables gives the results of a calculation in which relaxation was ignored. This affords a comparison with the SLA results given in Table I. The consequence of allowing the Al lattice to move is that all the values of ν_L increase. There are two causes for this. It can be seen from the tables that the value of $\bar{D}$ also increases, largely due to the addition of the inband contributions. This leads to a general increase in frequency. Also, it is a general result that on using the same force constants the SLA always underestimates ν_L. This difference becomes larger as the value of ν_L becomes smaller as then the Al ions take a greater part in the motion associated with the local mode. For the unrelaxed octahedral calculations the ratio of the dynamic to static values of ν_L is 1.05 for D, dropping to 1.02 for H. It can be seen that the SLA values are in quite good agreement with the dynamical results and that the SLA is quite sufficient to estimate these frequencies. We note that the ratio R_L, being a measure of anharmonicity, has now dropped to 1.09 for the octahedral case and to 0.98 for the tetrahedral case.

The second lines in Tables II and III give the results that were obtained when the relaxation was taken into account. These calculations were fully self-consistent but only a first-order solution for the relaxation equation was used. The outward NN relaxations reduce all the frequencies, with particularly strong reductions in the tetrahedral case. However the values of R_L are maintained at those quoted

TABLE II. Results of dynamical calculations for the octahedral site.

		Force constants (10^3 dyn cm^{-1})						Relaxations (Å)	
		NN		NNN					
Ion	ν_L(THz)	long	trans	long	trans	α	$\bar{D}^{1/2}$(Å)	NN	NNN
D	13.07	12.75	−2.77	0.60	0.69	3.42	0.154	. . .	. . .
	11.18	9.17	−2.56	1.03	−0.69	2.79	0.167	0.046	−0.013
	12.06	16.03	−4.26	. . .	. . .	1.64[a]	0.174	0.047	
	10.37	10.62	−2.66	. . .	. . .	0	0.183	0.048	
H	19.33	14.86	−2.94	0.71	0.72	3.05	0.174	. . .	. . .
	16.49	10.98	−2.68	1.06	−0.60	2.53	0.187	0.048	−0.012
	17.00	16.71	−3.97	. . .	. . .	1.46[a]	0.192	0.049	
	14.91	12.33	−2.78	. . .	. . .	0	0.201	0.050	

[a]NN scaling factor.

TABLE III. Results of dynamical calculations for tetrahedral site.

Ion	ν_L(THz) A	T_2	Force constants (10^3 dyn cm^{-1}) long	trans	α	$\bar{D}^{1/2}$ (Å)	Relaxation (Å)
	11.08	27.63	87.49	−9.50	1.09	0.126	...
	10.34	21.92	55.99	−6.41	1.14	0.132	0.083
D							
	10.27	21.33	53.15	−6.16	1.15	0.133	0.092[a]
	10.12	19.94	46.40	−5.38	0	0.135	0.093[a]
	11.15	38.63	90.44	−9.94	1.08	0.141	...
	10.38	30.68	57.75	−6.66	1.14	0.150	0.086
H							
	10.31	29.28	54.66	−6.39	1.14	0.151	0.096[a]
	10.16	27.95	48.10	−5.63	0	0.164	0.097[a]

[a]Iterated relaxation calculation.

above for the unrelaxed calculations.

The relative change in NN distance, as calculated in first order, is quite modest for the octahedral case being just over 2%. However, as this change increases to 5% for the tetrahedral case we extended the calculations by iterating the relaxation equation (9). The results are given in the third lines in Table III and they show further small decreases in the local mode frequencies. We did a similar calculation for the octahedral case and found, as expected, changes in ν_L of less than 1%.

At this stage we can safely state that for the octahedral case the different isotopes have such sufficiently different frequencies that an inverse isotope effect might be expected. Further the D local mode frequency is about 10% above the maximum Al frequency. For the tetrahedral case there is essentially no isotope effect to be expected on the basis of the frequencies calculated. However we have calculated a D local mode frequency that is about twice the maximum Al frequency. This is just the frequency region in which Kus and Carbotte[3] added an extra peak to $\alpha^2 f(\omega)$ in their calculations of the tunneling characteristic for Al-D. We have already discussed in the Introduction as to why this site might be appropriate for large D concentrations.

As the motivation for our calculations comes from measurements on the superconducting properties of Al-H,D it is natural that we use our dynamical results to calculate the changes in T_c. This we will do in Sec. IV but we can anticipate that this could need considerable computer time. To reduce this time for the octahedral case we have repeated some of our calculations taking into account just the NN force constants. The results are shown on the third lines in Table II. The rather large scaling of the force constants (FC) should be noted as well as the increase in the local mode frequency. More serious is the reduction in R_L to unity. A comparison of the FC's for D and H indicates that although the magnitude of the longitudinal FC increases in going from D to H, the magnitude of the transverse FC decreases contrary to all other NN entries in Tables II and III. As this behavior might be an artefact of our scaling procedure we repeated the calculation with no scaling. The results are given in the fourth lines of Table II. The local mode frequencies have dropped, as expected, but R_L has now risen to 1.04. This is still smaller than the NNN results but gives some hope for an inverse isotope effect. A similar calculation was also done for the tetrahedral case and is reported in the fourth lines of Table III.

It is of some interest to examine the various contributions to $\bar{D}$. This is done in Table IV for one case, that of H at an octahedral site using the force constants given in line 2 of Table II. It is not surprising that the local mode motion of H ion gives the dominant contribution. However, the inband motions of the H and Al ions are comparable and

TABLE IV. Displacement-displacement correlation functions for octahedral H and a NN Al in the [100] direction (10^{-3} Å^2).

	$\langle u_x^H u_x^H \rangle$	$\langle u_x^H u_x^{Al} \rangle$
Inband	1.10	0.670
Local mode	8.08	−0.232
Total	9.18	0.438

$\langle u_y^H u_y^{Al} \rangle$	$\langle u_x^{Al} u_x^{Al} \rangle$	$\langle u_y^{Al} u_y^{Al} \rangle$
−0.053	0.896	0.966
0.068	0.007	0.001
0.015	0.903	0.967

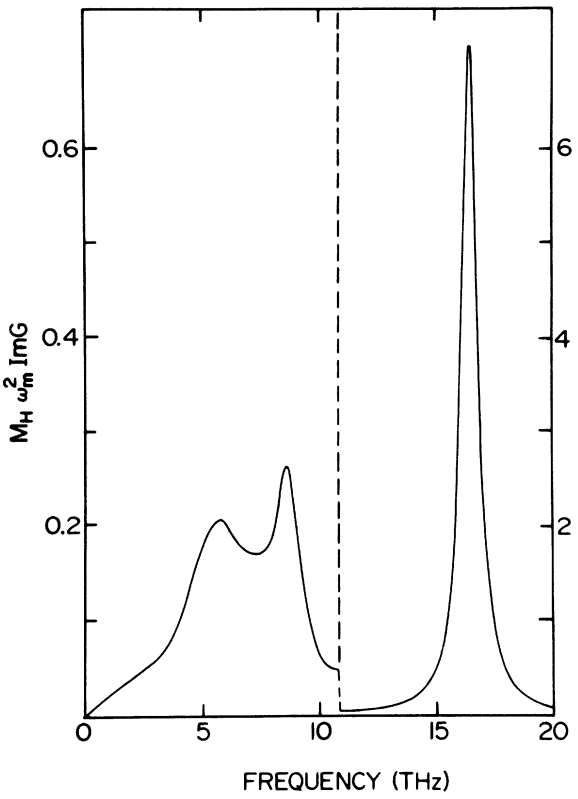

FIG. 2. $M_H\omega_m^2\,\mathrm{Im}G_{xx}(i,i;\omega-i\delta)$ for octahedral H, using force-constant scaling and $\delta=0.4$ THz, as a function of frequency ($\nu_m=10$ THz). Note that beyond $\nu=10.8$ THz the vertical scale has been decreased by a factor of 10.

further, the H-Al correlation is quite significant. This general division of strength between the various contributions is fairly typical of the results found in the other cases evaluated. In fact this case has the largest dominance of the H local mode contribution. More typically the ratio is 3:1 rather than the 7:1 of this case. Considerable in-band motion of an interstitial has also been found by Lottner *et al.*[10] for H at tetrahedral sites in bcc metals.

The dominant contribution of the local mode to the H motion is further illustrated in Fig. 2 where we plot the integrand of Eq. (13) for $l=l'=i$ and $\alpha=\beta$ as a function of frequency. Following the procedure used later in Sec. IV the imaginary part of the Green's function was calculated at a finite distance $\delta=0.4$ THz off the real axis. As a consequence the local mode δ function now has a finite width. Aside from corrections due to diffusive motion[10] this figure indicates what should be expected in an inelastic incoherent neutron scattering experiment.

IV. CHANGES IN THE SUPERCONDUCTING TRANSITION TEMPERATURE

A. Theory

On alloying the superconducting transition temperature is changed by both the electron-impurity scattering and by any modifications to the electron-phonon interaction. The electron-phonon interaction enters superconductivity calculations via the function $\alpha^2F(\omega)$.[27] This has the form of a phonon density of states weighted by the electron-phonon interaction. For weak coupling superconductors Leavens and Carbotte[28] have given a good approximate formula for T_c that includes electron-phonon anisotropy. $\alpha^2F(\omega)$ enters their formula via the integrals

$$\lambda=2\int\frac{d\omega}{\omega}\alpha^2f(\omega)\ ,$$
$$\bar{\lambda}=2\int\frac{d\omega}{\omega}\alpha^2f(\omega)\ln(1+\omega_m/\omega)\ , \tag{22}$$

where ω_m is the maximum phonon frequency. The anisotropies in λ and $\bar{\lambda}$ are described by two quantities $\langle ab\rangle$ and $\langle a\bar{b}\rangle$ which they have determined, for Al, to be 0.0081 and 0.0142, respectively. The electron-impurity scattering tends to wash out the effects of such anisotropy and Markowitz and Kadanoff[29] have shown how, in a BCS approximation, an inverse collision time τ^{-1}, can be used to describe this behavior.

Recently, Kus,[30] has amalgamated these methods and has found corrections, in terms of λ, to the result of Markowitz and Kadanoff. Although Kus did not include changes in $\alpha^2f(\omega)$ his method can be readily modified to include such changes.[31] The result is that the change in transition temperature ΔT, from the pure Al transition temperature T_c is given by

$$1+\lambda_a+\bar{\lambda}_a+\langle ab\rangle\lambda_a(1-I)+\langle a\bar{b}\rangle[\bar{\lambda}_a+\lambda_a(I-I_\lambda)]=[\lambda_a(1+\langle ab\rangle)-\mu^*][\ln(1.134\hbar\omega_m/k_BT_c)-\Delta T/T_c]\ . \tag{23}$$

The subscript a refers to quantities calculated for the alloy. The collision time τ enters in the integrals

$$I=\int\frac{d\omega}{\omega}\tanh\left(\frac{\hbar\omega}{2k_BT_c}\right)(1+\omega^2\gamma^2)^{-1} \tag{24}$$

(this is the same as the integral I of Markowitz and Kadanoff) and

$$I_\lambda = \int \frac{d\omega}{\omega} \tanh\left(\frac{\hbar\omega}{2k_B T_c}\right)(1+\omega^2\gamma^2)^{-1}\frac{\lambda_a(\omega)}{\lambda_a} \quad . \tag{25}$$

Here $\gamma = 2\tau(1+\lambda)$ and $\lambda_a(\omega) = 2\int d\omega' \alpha^2 f(\omega')_a/(\omega+\omega')$. In the pure limit ($\gamma \to \infty$) both I and I_λ are zero and we can use Eq. (23) to determine the electron-electron pseudopotential μ^* from the known values of λ, $\bar{\lambda}$, and T_c. In the dirty limit ($\gamma \to 0$), $I_\lambda - I \to \bar{\lambda}_a/\lambda_a$ and the $\bar{\lambda}$ anisotropy is removed. However the anisotropy in λ is not removed.

There remains the calculation of $\alpha^2 f(\omega)$ and τ within the approximations of the previous sections. For an alloy $\alpha^2 f(\omega)$ is conveniently given by[9]

$$\alpha^2 f(\omega) = \frac{N(0)s(\omega)}{8\pi^2 k_F^2 N^2}\int_{k<2k_F}\frac{d^3k}{k}\sum_{ll',\alpha\beta}\bar{w}_l(k)k_\alpha \mathrm{Im}G_{\alpha\beta}(ll';\omega)k_\beta \bar{w}_{l'}(k)\exp\{i\vec{k}\cdot[\vec{R}(l)-\vec{R}(l')]\} \quad . \tag{26}$$

Here $N(0)$ is the single spin density of states for the Al alloy and $\bar{w}_l(k)$ is the screened form factor for the ion at $\vec{R}(l)$. The factor

$$s(\omega) = \begin{cases} 5\omega/\omega_m \ , & \omega \leq \frac{1}{5}\omega_m \\ 1 \ , & \omega > \frac{1}{5}\omega_m \end{cases} \tag{27}$$

has been introduced to compensate for the fact that the form of Eq. (26) is based on a single, rather than a multiple orthogonalized plane wave (OPW), calculation of the electron-phonon interaction.[32] On using the approximation in Eq. (18) for G, Eq. (26) naturally splits into four terms

$$\alpha^2 f(\omega) = \alpha^2 f(\omega)_{\mathrm{Al}} + \Delta\alpha^2 f(\omega)_{\mathrm{Al}} + \Delta\alpha^2 f(\omega)_{\mathrm{Al},I} + \Delta\alpha^2 f(\omega)_I \quad . \tag{28}$$

The first term, $\alpha^2 f(\omega)_{\mathrm{Al}}$, is not affected by the changed lattice dynamics. However it is not the same as the pure Al function for two reasons. First, the addition of the interstitial ions changes the electron density and hence k_F and $N(0)$. Second, because the $\vec{R}(l)$ in Eq. (26) refer to the equilibrium ionic positions, relaxation effects should be considered (see Appendix). As we are working to first order in the fractional concentration c (i.e., the number of interstitial ions per Al ion) these two effects can be considered independently.

Carbotte *et al.*[33] have given a simple expression with which to calculate the change in λ for a change in the electron density in Al. For a univalent impurity it is

$$\Delta\lambda/\lambda = 0.22c \quad . \tag{29}$$

We assumed that $\bar{\lambda}$ obeys the same relation.

The second term in Eq. (28) describes the changes in $\alpha^2 f(\omega)$ due to the modification of the Al dynamics. It can be written as

$$\alpha^2 f(\omega)_{\mathrm{Al}} = \frac{cN(0)}{8\pi^2 k_F^2}\int\frac{d^3k}{k}\frac{1}{N^2}\sum_{ll',\alpha\beta}\bar{w}_{\mathrm{Al}}(k)k_\alpha \mathrm{Im}\sum_{l_i l_i',\gamma\delta}P_{\alpha\gamma}(l,l_i';\omega)T_{\gamma\delta}(l_i,l_i';\omega)$$
$$\times P_{\delta\beta}(l_i'l';\omega)k_\beta \bar{w}_{\mathrm{Al}}(k)\exp\{i\vec{k}\cdot[\vec{R}(l)-\vec{R}(l')]\} \quad . \tag{30}$$

Here l and l' refers to Al lattice sites, l_i and l_i' refer to the NN of an interstitial. The screened Al form factor $\bar{w}_{\mathrm{Al}}$, was calculated using the pseudopotential given in Sec. II A being screened according to Vashishta and Singwi.[34] Equation (30) can be simplified somewhat to read

$$\Delta\alpha^2 f(\omega)_{\mathrm{Al}} = \frac{cN(0)}{8\pi^2 k_F^2 M^2 N}\int\frac{d^3k}{k}\bar{w}_{\mathrm{Al}}(k)^2\sum_{j_1 j_2}\vec{k}\cdot\vec{\sigma}^{j_1}(k)\,\mathrm{Im}P_{j_1}(\vec{k},\omega)T_{j_1 j_2}(\vec{k},\omega)P_{j_2}(\vec{k},\omega)\vec{k}\cdot\vec{\sigma}^{j_2}(\vec{k}) \quad , \tag{31}$$

with

$$T_{j_1 j_2}(\vec{k},\omega) = \sum_{sab\lambda} S(\vec{k},j_1;s,a,\lambda)T_{ab}(s,\omega)S^*(\vec{k},j_2;sb\lambda) \quad , \tag{32}$$

where

$$S(\vec{k},j;sa\lambda) = \sum_{l_i\alpha}\sigma_\alpha^j(\vec{k})e^{-i\vec{k}\cdot\vec{R}^0(l_i)}\psi_\alpha^{(sa\lambda)}(l_i) \quad . \tag{33}$$

All the phonon quantities and the transformation matrices ψ are described in Sec. II D.

Although $N(0)$ and k_F should have values appropriate to the alloy electron density we used the pure Al values in this and the next two terms. This should be an error of order c on a term that is already of order c.

The third term in Eq. (28) results from the correlation between the Al and the interstitial motion. It can be reduced to the form

$$\alpha^2 f(\omega)_{\mathrm{Al},I} = \frac{cN(0)}{8\pi^2 k_F^2 M M_I N} \int \frac{d^3k}{k} \bar{w}_{\mathrm{Al}}(k)\bar{w}_I(k) \sum_{j\beta b} \vec{k}\cdot\vec{\sigma}^j(\vec{k})\,\mathrm{Im}P_j(\vec{k},\omega)T_{1b}(s,\omega)\omega^{-2}k_\beta[2\,\mathrm{Re}S(\vec{k},j;sb\beta)] \quad . \tag{34}$$

In the octahedral case the interstitial motion has just T_{1u} symmetry and in the choice of ψ that we used only the $a=1$ component is needed. Hence, in Eq. (34), $s \equiv T_{1u}$. Similarly for the tetrahedral case, it is just the T_2 representation that appears in Eq. (34). In order to calculate the screened interstitial form factor we used the same nonlinear result for the screening cloud electron density $n(r)$ as was used to calculate the interstitial-Al potential in Sec. II A. Hence

$$\bar{w}_I(k) = (4\pi e^2/k^2)[n(k)-1]\exp[-\tfrac{1}{2}k^2\langle u_x(i)^2\rangle] \quad . \tag{35}$$

Note that we have included the Debye-Waller factor,[35] which is quite significant even at low T.

The two form factors used are shown in Fig. 3. The interstitial form factor $\bar{w}_I$ at $q=0$ can be seen to be about a half the value expected from linear screening theory which is a third of the value of $\bar{w}_{\mathrm{Al}}$. However the two form factors become similar as q approaches $2k_F$, the region that is most strongly weighted in the integral in Eq. (26) for $\alpha^2 f(\omega)$.

The final term, $\Delta\alpha^2 f(\omega)_I$, in Eq. (28) is the direct interstitial contribution to $\alpha^2 f(\omega)$ and takes the form

$$\Delta\alpha^2 f(\omega)_I = \frac{cN(0)}{8\pi^2 k_F^2 M_I^2 N}\,\mathrm{Im}\,\frac{1}{\omega^2}\,T'_{II}(s,\omega) \times \int_{k<2k_F} \frac{d^3k}{k}\,\bar{w}_I(k)^2 \quad , \tag{36}$$

where

$$T' = (1-PC')^{-1} \quad .$$

Again for the octahedral and tetrahedral cases $s \equiv T_{1u}, T_2$, respectively.

The above integrals over $\vec{k}$ were handled by the procedure of Carbotte and Dynes.[36] As the calculation of the integrands is rather time consuming we used a fairly coarse mesh of 112 $\vec{k}$ points in the reduced $\frac{1}{48}$th of the first Brillouin zone. In order to calculate the imaginary parts of the Green's function we evaluated them a finite distance δ off the real axis. This has the advantage of eliminating some of the noise due to the coarse $\vec{k}$ mesh. We finally chose a somewhat large value of $\delta = 0.04\omega_m$ which removed most of the noise without producing tails of too great an extent.

In the absence of the correction factor $s(\omega)$ in Eq. (26) it is possible to calculate λ directly. As Taylor and Vashishta[37] have shown, λ can be written as

$$\lambda = \frac{N(0)}{8\pi k_F^2}\int_{k<2k_F}\frac{d^3k}{k}\frac{1}{N^2}\sum_{II',\alpha\beta}\bar{w}_I(k)k_\alpha\Phi^{-1}_{\alpha\beta}(II')k_\beta\bar{w}_{I'}(k) \times\exp\{i\vec{k}\cdot[\vec{R}(I)-\vec{R}(I')]\} \tag{37}$$

and $\Phi^{-1} = -G(\omega=0)$. Hence, λ can be calculated using the above procedure, but without the time consuming need to repeat the procedure for a large number of frequencies. This allowed us to do the $\vec{k}$ integral over a much finer mesh of $\vec{k}$ points. In fact we found that extending the number of points from 112 to 615 produced changes in $\Delta\lambda$ of less than 1% [$\Delta\lambda$ is the contribution to λ due to the last three terms in Eq. (28)]. We also found that the value of $\Delta\lambda$ determined by numerically integrating Eq. (26) with $s(\omega)=1$ was within 3% of these values. Hence, we have considerable confidence in the accuracy of the numerical methods.

The effects of relaxation can also be estimated using this expression for λ. As they turned out to be

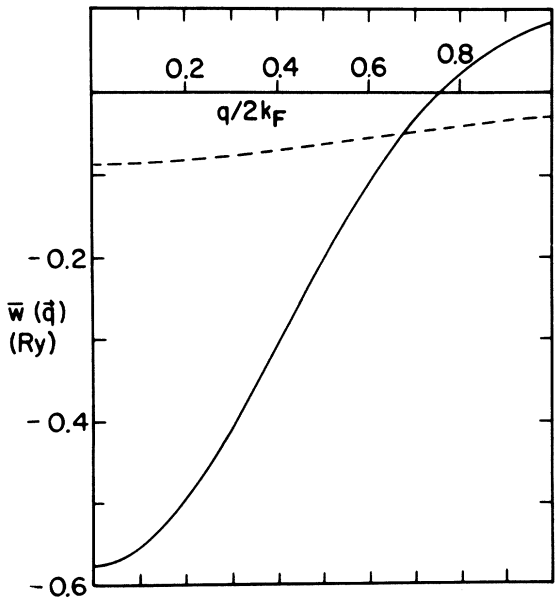

FIG. 3. The screened form factor $\bar{w}(q)$ for Al (——) and H (– – – – – –).

small this aspect of the calculations is described in the Appendix.

The golden rule result for inverse lifetime, to first order in c, is given by

$$\tau^{-1}=\frac{N(0)}{8N\hbar k_F^4}\int d^3kk\sum_{ll'}\bar{w}_l(k)\bar{w}_{l'}(k)\exp\{i\vec{k}\cdot[\vec{R}(l)-\vec{R}(l')]\}=\frac{cN(0)}{8\hbar k_F^4}\int d^3kk[\bar{w}_l(k)+\bar{w}(k)\Delta S(k)]^2 \ , \quad (38)$$

with

$$\Delta S(k)=\sum_l (e^{i\vec{k}\cdot\vec{R}(l)}-e^{i\vec{k}\cdot\vec{R}^0(l)})e^{-i\vec{k}\cdot\vec{R}(i)} \ . \quad (39)$$

The sum over l refers only to the NN and NNN sites of a given interstitial site $\vec{R}(i)$. No long-range relaxation was considered and indeed we found the effects of the NNN relaxation to be negligible.

B. Results

The values of the various contributions to $\Delta\lambda$ for D ions at octahedral sites are given in Table V for the case of force-constant scaling. In the rest of this section the results of scaling or not scaling the force constants will be indicated by FS and NFS, respectively. These values require multiplication by c. For comparison, the value of λ for Al is 0.432. Due to the low value of the local mode frequency and the relatively large value of δ, the inband and local mode contributions to $\Delta\alpha^2f(\omega)$ overlap, as can be seen in Fig. 4. To produce the inband and local mode values in Table V the local mode contribution was calculated exactly from the residue of the t matrix as $\delta\rightarrow 0$ and then subtracted from the total $\Delta\lambda$.

The contributions due to the correlation between the Al and D motions [Eq. (34)] are of particular significance. The total inband contribution is reduced almost to zero due to this term leading to an almost complete dominance by local mode contribution. This is a somewhat surprising result considering that the weak interstitial pseudopotential (Fig. 3) could be expected to suppress the large local mode displacement (Fig. 2). Further, it is the large value of this term that prevents an analysis of our results following the method of Papaconstantopoulus *et al.*[26] They assumed two separate contributions to λ, one from the host ion dominating the acoustic branches and the other from the interstitial ions dominating the optical branches. In our dilute interstitial situation it is not true that the inband contribution is dominated by the Al motion and the local mode contribution by the light interstitial motion.

In Table VI we compare the contributions to $\Delta\lambda$ and ΔA to H and D interstitials again for the FS case. ΔA is the change in the area under $\alpha^2f(\omega)$, the area for Al being 1.43 THz. This comparison clearly shows that although the interstitial H produces the greater increase in $\alpha^2f(\omega)$, the ω^{-1} weighing in λ leads to the interstitial D producing the larger change in λ. It is this behavior that leads to an inverse isotope effect in this system. According to Eq. (37) λ does not depend explicitly on the atomic masses and hence any differences between $\Delta\lambda$ for H and for D can only come from different force constants and different values of $\langle u^2\rangle$. [This mass independence is maintained to within 1% even when the multi-OPW

TABLE V. Contributions to $\Delta\lambda$ due to an octahedral D in (FS, $c=1$).

		$\Delta\lambda_{Al}$	$\Delta\lambda_{Al/D}$	$\Delta\lambda_D$	$\Delta\lambda$
	Inband	0.150	−0.616	0.525	0.059
D	Local mode	0.063	0.103	0.240	0.406
	Total	0.213	−0.513	0.765	0.465

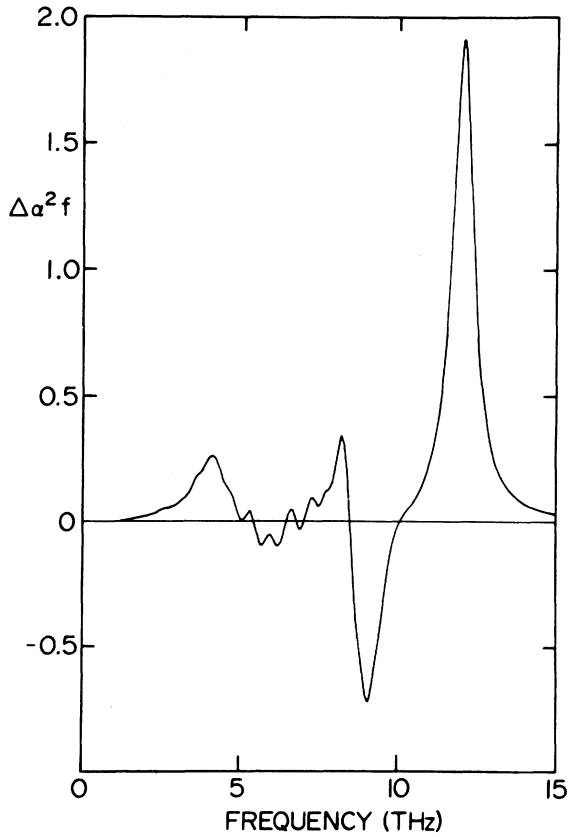

FIG. 4. $\Delta\alpha^2f(\omega)$ as a function of frequency for octahedral D using force-constant scaling.

TABLE VI. Comparison between changes in λ and A for an octahedral interstitial (FS, $c=1$).

	$\Delta\lambda$	ΔA (THz)	$\Delta\lambda$	ΔA (THz)
Inband	0.059	−0.36	−0.020	−0.45
Local mode	0.406	2.45	0.351	2.98
Total	0.465	2.09	0.331	2.53

TABLE VII. Anharmonic and Debye-Waller factor contributions to $\Delta\lambda$, see text for notation (FS, $c=1$).

	$\langle u_x^2\rangle_D$	$\langle u_x^2\rangle_H$
Φ_D	0.465	0.440
Φ_H	0.351	0.331

correction, $s(\omega)$ is included, as in Eq. (26).] To investigate this point we constructed the matrix in Table VII. There we give values for $\Delta\lambda$ due to different combinations of the values of $\langle u_x^2(i)\rangle$ and the force constants appropriate to D($\langle u_x^2\rangle_D, \Phi_D$) and H($\langle u_x^2\rangle_H, \Phi_H$) in the FS case. It can be seen that the difference between $\Delta\lambda$ for D and for H is dominated by the force-constant difference arising from the anharmonic corrections described in Sec. II B. This is also the case when the values appropriate to the NFS case are used.

The situation for $\bar{\lambda}$ is somewhat more complicated as it does depend upon the atomic masses. We found that $\Delta\bar{\lambda}$ increases by about 30% if the H parameters are used along with the D mass. Indeed it is this behavior that leads to an isotope effect in the normal direction if T_c is calculated using the method described in Sec. IV A. The results of a set of calculations similar to those described above for $\Delta\lambda$ indicate that again it is the anharmonic change in the force constants that is the main reason for $\Delta\bar{\lambda}$ being smaller for H than for D.

Our values of $\Delta\lambda$ and $\Delta\bar{\lambda}$ are presented in Table VIII. It can be seen that in the octahedral case the H values of $\Delta\lambda$ and $\Delta\bar{\lambda}$ are smaller than the D values whether or not force constant scaling is used. This leads to our feeling confident about this prediction of an inverse isotope effect.

Results of the tetrahedral case are also given in Table VIII. Only small changes in $\Delta\lambda$ and $\Delta\bar{\lambda}$ are predicted leading to a prediction of essentially no isotope dependence of T_c. An analysis similar to that which produced Table VII indicates that the increase in force constants in going from D to H leads to an increase in $\Delta\lambda$ contrary to the octahedral case. Preliminary lattice dynamic calculations indicated that for very large interstitial-Al force constants a low-frequency resonance can occur in the T_{1u} mode. Presumably this increase in $\Delta\lambda$ is due to an incipient resonance of this kind.

In order to calculate the changes in T_c via Eq. (23) values of τ^{-1} from Eq. (38) are required. The values we found for τ^{-1} ranged from 0.481 THz (NFS, tetrahedral H) to 0.604 THz (FS, octahedral D) for 1% of the interstitial ions. The corresponding residual resistivities range from 0.0093 $\mu\Omega$ cm to 0.0117 $\mu\Omega$ cm. It should be noted that we found the inclusion of relaxation lead to a reduction of τ^{-1} by about 40%.

The resulting fractional changes in T_c, $\Delta T/T_c$, are shown in Fig. 5 for the octahedral case. Experimentally, it is commonly found that $\Delta T/T_c$ is initially negative due to the impurity scattering removing the anisotropy in the electron-phonon interaction. However there are examples [e.g., Ga in In (Ref. 38)] for which $\Delta T/T_c$ is always positive. That $\Delta T/T_c$ is predominantly positive in our case is due to a weak impurity scattering with the change in $\Delta T/T_c$ being

TABLE VIII. Dynamical changes in λ and $\bar{\lambda}$ calculated with and without the force-constant scaling correction ($c=1$).

	FS		NFS	
	$\Delta\lambda$	$\Delta\bar{\lambda}$	$\Delta\lambda$	$\Delta\bar{\lambda}$
Octahedral				
D	0.465	0.429	0.540	0.453
H	0.331	0.216	0.376	0.207
Tetrahedral				
D	0.458	0.619	0.435	0.555
H	0.464	0.608	0.438	0.538

dominated by $\Delta\lambda$ and $\Delta\bar{\lambda}$. To illustrate this we show in Fig. 5 the result of doubling τ^{-1} for H(FS). The result is that $\Delta T/T_c$ is negative for an appreciable range of concentrations. This calculation also serves to indicate the effect of the presence of other scattering mechanisms. These are to be expected in samples prepared by ion implantation.

In Fig. 5 the curves of $\Delta T/T_c$ for D lie well above those for H, whether or not force-constant scaling is taken into account. In particular, at $c=0.01$ the value of $\Delta T/T_c$ for D is 40% greater than that for H. This confirms the inverse isotope effect suggested by the dynamical results of Sec. III and is, of course, as expected from the results given in Table VIII. To compare these results for $\Delta T/T_c$ with those from a harmonic approximation we calculated $\Delta T/T_c$ using H forces and potentials but the D mass. The result was that $\Delta T/T_c$ at $c=0.01$ was 10% lower (due to changes in $\Delta\bar{\lambda}$) than when the H mass was used, provided the valence effect, Eq. (29), was omitted. Otherwise the change was then less than 1%.

There is not much difference between the values of $\Delta T/T_c$ for any of the tetrahedral cases. Hence, we show in Fig. 6 just the results for H(FS) which has the largest $\Delta T/T_c$ and the results for D(NFS) which has the smallest $\Delta T/T_c$. As expected from Table VIII no inverse isotope effect is to be expected and in fact our results indicate that at $c=0.01$ the value of $\Delta T/T_c$ for D is 4% lower than the value for H. It will be noted that these values of $\Delta T/T_c$ for tetrahedral interstitials are quite similar to those for the octahedral interstitials.

The validity of Leavens and Carbotte's[28] approximation might be questioned, particularly as no

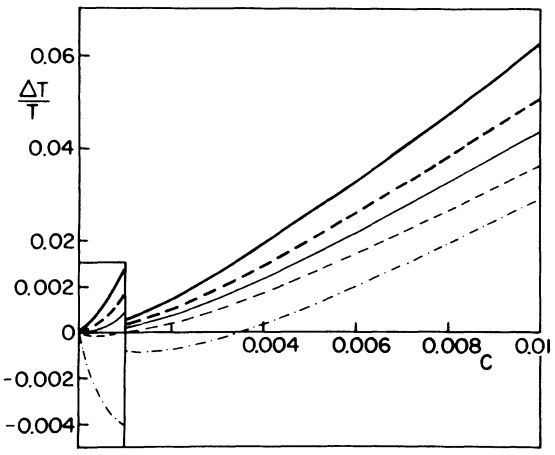

FIG. 5. Fractional change of the superconducting transition temperature $\Delta T/T$ as a function of the fractional concentration c of octahedral interstitial ions. —— D(NFS), – – – – – – D(FS), —— H(NFS), – – – – – – H(FS), —·—·— H(FS) with a doubled value of τ^{-1}.

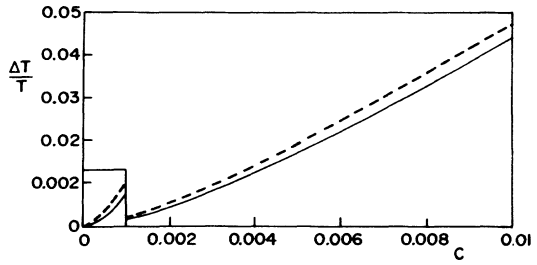

FIG. 6. Fractional change of the superconducting transition temperature $\Delta T/T$ as a function of the fractional concentration c of tetrahedral interstitial ions. —— D(NFS), – – – H(FS).

changes were made in the ω_m in Eq. (23). To this end the Eliashberg equations were solved for T_c (Ref. 39) in the isotropic approximation[40] using the $\delta\alpha^2 f(\omega)$ for H and D (NFS). These exact solutions gave values of $\Delta T/T_c$ that differ by less than 2% from those obtained from the isotropic version of Eq. (23).

V. CONCLUSION

Our various calculations of the local mode frequency for interstitial H and D in Al clearly indicate that a local mode is to be expected. On the assumption that at low concentrations the interstitials are at octahedral sites the local mode frequency for H can be expected to be well above the maximum Al phonon frequency whereas for D our results indicate that these two frequencies differ by about only 10%. A high local mode frequency is predicted for both H and D at tetrahedral sites and on the assumption that this frequency is a measure of the position of the impurity band at large concentrations, our results indicate a very high frequency for this band. As there are other strong contributions to tunneling characteristics at such frequencies this explains why such a band has not yet been observed in tunneling experiments. It would be of considerable interest if inelastic neutron scattering experiments were to be carried out on these systems, at both low and high interstitial concentrations.

When our dynamical results are used to calculate the changes in the superconducting transition temperature T_c a very definite inverse isotope is predicted for octahedral interstitial. We found that at $c=0.01$ the fractional change in T_c due to D is about 40% greater than that due to H in spite of the fact that the local mode frequencies show only weak anharmonic effects. Further, as the lattice dynamics calculations show larger anharmonic effects if the NNN forces are included (Table II), it can be presumed that our NN results underestimate the inverse isotope effect. However, there is very little

difference between the H and D results for the tetrahedral case, there being a weak isotope effect in the normal direction. The results of an experimental investigation of the effects on T_c of low concentrations of H and D in Al would be of considerable interest.

The tetrahedral results are in qualitative agreement with the experimental results at large concentrations[2] in that they also show an isotope effect in the normal direction. To examine these experimental results further our next calculations should be to examine the large-concentration situation. A first stage in doing this would be to calculate the properties of an ordered alloy based on the same kind of initial data as was used in these low-concentration calculations.

ACKNOWLEDGMENTS

I wish to thank Dr. J. P. Carbotte for drawing to my attention the experiments on Al-H,D and for subsequent discussions. I have also benefitted from many discussions with Dr. F. W. Kus and from the use of his approximation for T_c prior to publication. This work was supported by the National Science and Engineering Research Council of Canada.

APPENDIX

In calculating the effects of relaxation on $\alpha^2 f(\omega)$ the important part of Eq. (26) is

$$K = \sum_{ll'} K(l,l') = \sum_{ll'} e^{i\vec{k}\cdot\vec{R}(l)} G_{\alpha\beta}(l,l') e^{-i\vec{k}\cdot\vec{R}(l')} \quad . \tag{A1}$$

Any derivation of the electron-phonon coupling Hamiltonian shows that the exponential factors in Eq. (A1) originate from taking electron matrix elements of the electron ion potential $V(\vec{r})$ with $\vec{r}=\vec{r}_e - \vec{R}(l)$. Here $\vec{r}_e$ is an electron coordinate and $\vec{R}(l)$ the instantaneous position of the ion at site l. Hence, after the usual expansion for the thermal displacements about equilibrium the $\vec{R}(l)$ that survives in Eq. (A1) is the equilibrium position and is subject to relaxation from its value in pure Al.

As we take into account the relaxation of just the nearest neighbors of the interstitial ions, the site sums in Eq. (A1) can be conveniently divided up in the following manner:

$$K = \sum_{l \notin \{s_i\}} \sum_{l' \notin \{s_i\}} + \sum_{is_i} \sum_{l \notin \{s_i\}} K_{r0}(s_i,l) + \sum_{l \in \{s_i\}} \sum_{js_j} K_{0r}(l,s_j) + \sum_{is_i} \sum_{js_j} K_{rr}(s_i,s_j) \quad . \tag{A2}$$

Here $\{s_i\}$ stands for the set of all sites in the defect spaces of the interstitials which are at sites i and the subscripts of K indicate whether (r) or not (0) a site is relaxed.

By adding and subtracting terms the restrictions on the summations can be removed to give

$$\begin{aligned} K = & \sum_{ll'} K_{00}(l,l') \\ & + \sum_{is_j} \sum_{l} [K_{r0}(s_i,l) - K_{00}(s_i,l)] \\ & + \sum_{l} \sum_{js_j} [K_{0r}(l,s_j) - K_{00}(l,s_j)] \\ & + \sum_{is_j} \sum_{js_j} [K_{rr}(s_i,s_j) - K_{0r}(s_i,s_j) \\ & \qquad - K_{r0}(s_i,s_j) + K_{00}(s_i,s_j)] \quad . \end{aligned} \tag{A3}$$

The first term refers to the unrelaxed case and has been calculated in Sec. IV. The remaining terms then give the relaxation correction.

As all calculations are being done to first order in c the explicit interstitial sites in Eq. (A3) must coincide with the interstitial sites that appear in the approximation (18) for the Green's function in Eq. (A1). The resulting approximation for the second term is

$$\sum_{is_i s_i', \gamma} \Delta S(\vec{k},s_i) T'_{\alpha\gamma}(s_i s_i') \exp\{-i\vec{q}\cdot[\vec{R}^0(s_i') - \vec{R}(i)]\} P_{\gamma\beta}(\vec{k}) \quad ,$$

where

$$\Delta S(\vec{k},s_i) = [e^{i\vec{k}\cdot\vec{R}(s_i)} - e^{i\vec{k}\cdot\vec{R}^0(s_i)}] e^{-i\vec{k}\cdot\vec{R}(i)}$$

and $P_{\gamma\beta}(\vec{k})$ is the Fourier transform of $P_{\gamma\beta}(l,l')$. The third term gives an equal contribution.

For the fourth term, again all the explicit and implicit interstitials sums must be replaced by one sum to give

$$\sum_{is_i s_i'} \Delta S(\vec{k},s_i) Q_{\alpha\beta}(s_i s_i') \Delta S(\vec{k},s_i')^* \quad ,$$

where $Q = (1 - PC^i)^{-1} P$.

All these correction terms contribute to $\Delta\alpha^2 F(\omega)_{\rm Al}$ (Eq. 28). However only the second and third terms in Eq. (A3) contribute $\Delta\alpha^2 f(\omega)_{{\rm Al},l}$ with the restriction that $l = i$. There are no relaxation corrections to $\Delta\alpha^2 f(\omega)_l$.

As a time-saving preliminary calculation these equations were used to calculate the corrections to λ via the sum rule Eq. (37). Changes of 0.2% and -0.4% were found for the octahedral and tetrahedral cases (D,NFS), respectively. As these values are insignificant no further calculations were done.

[1]A. M. Lamoise, J. Chaumont, F. Meunier, and H. Bernas, J. Phys. (Paris) Lett. 36, 271 (1973).
[2]L. Dumoulin, P. Nédellec, J. Chaumont, D. Gilbon, A. M. Lamoise, and H. Bernas, C. R. Acad. Sci., P Ser. B 283, 285 (1976).
[3]F. W. Kus and J. P. Carbotte, Solid State Commun. 29, 715 (1979).
[4]For recent reviews see *Hydrogen in Metals, Topics in Applied Physics*, edited by G. Alefeld and J. Völkl (Springer-Verlag, New York, 1978), Vols. 28 and 29.
[5]Z. D. Popović, M. J. Stott, J. P. Carbotte, and G. R. Piercy, Phys. Rev. B 13, 590 (1976).
[6]W. Kohn and L. Sham, Phys. Rev. 140, A1133 (1965).
[7]N. S. Gillis, N. R. Werthamer, and T. R. Koehler, Phys. Rev. 165, 951 (1968).
[8]N. Singh, V. K. Jindal, and K. N. Pathak, Phys. Rev. B 18, 3271 (1978).
[9]For a review see, D. W. Taylor, in *Dynamical Properties of Solids*, edited by G. K. Horton and A. A. Maradudin (North-Holland, Amsterdam, 1974), Vol. 2, p. 287.
[10]V. Lottner, H. R. Schober, and W. J. Fitzgerald, Phys. Rev. Lett. 42, 1162 (1979).
[11]B. N. Ganguly, Z. Phys. 265, 433 (1973); Z. Phys. B 22, 127 (1975).
[12]R. J. Miller and C. B. Satterthwaite, Phys. Rev. Lett. 34, 144 (1975).
[13]D. S. Larsen and J. K. Nørskov, J. Phys. F 9, 1975 (1979).
[14]J. P. Bugeat, A. C. Chami, and E. Ligeon, Phys. Lett. A 58, 127 (1976).
[15]L. Sham, in *Modern Solid State Physics*, edited by R. H. Enns and R. R. Haering (Gordon and Breach, New York, 1969), Vol. 2, p. 143.
[16]A. Zunger and M. L. Cohen, Phys. Rev. B 18, 5447 (1978).
[17]H. Horner, in *Dynamical Properties of Solids*, edited by G. K. Horton and A. A. Maradudin (North-Holland, Amsterdam, 1974), Vol. 1, p. 453.
[18]H. Kanzaki, J. Phys. Chem. Solids 2, 24 (1957).
[19]A. A. Maradudin, E. W. Montroll, G. H. Weiss, and I. P. Ipatova, Solid State Phys., Suppl. 3, 420 (1971).
[20]A. A. Maradudin, Rep. Prog. Phys. 28, 331 (1965).
[21]P. Jena and K. S. Singwi, Phys. Rev. B 17, 3518 (1978); J. K. Nørskov, *ibid.* 20, 446 (1979).
[22]E. G. Brovman and Yu. M. Kagan, in *Dynamical Properties of Solids*, edited by G. K. Norton and A. A. Maradudin (North-Holland, Amsterdam, 1974), Vol. 1, p. 193.
[23]G. Gilat and L. J. Raubenheimer, Phys. Rev. 144, 390 (1966).
[24]G. Gilat and R. M. Nicklow, Phys. Rev. 143, 487 (1966).
[25]A. Rahman, K. Skold, C. Pelizzari, and S. K. Sinha, Phys. Rev. B 14, 3630 (1976).
[26]D. A. Papaconstantopoulus, B. M. Klein, E. N. Economou, and L. L. Boyer, Phys. Rev. B 17, 141 (1978).
[27]D. J. Scalapino, in *Superconductivity*, edited by R. D. Parks (Marcel Dekker, New York, 1969), p. 449.
[28]C. R. Leavens and J. P. Carbotte, Can. J. Phys. 49, 724 (1971); Ann. Phys. 70, 338 (1972).
[29]D. Markowitz and L. P. Kadanoff, Phys. Rev. 131, 563 (1963).
[30]F. W. Kus, Solid State Commun. 26, 411 (1978).
[31]F. W. Kus (unpublished).
[32]P. B. Allen and M. L. Cohen, Phys. Rev. B 1, 1329 (1970); H. K. Leung, J. P. Carbotte, D. W. Taylor, and C. R. Leavens, Can. J. Phys. 54, 1585 (1976).
[33]J. P. Carbotte, P. T. Truant, and R. C. Dynes, Can. J. Phys. 48, 1504 (1970).
[34]P. Vashishta and K. S. Singwi, Phys. Rev. B 6, 875 (1972).
[35]A. E. Karakozov and E. G. Maksimov, Sov. Phys. JETP 47, 358 (1978).
[36]J. P. Carbotte and R. C. Dynes, Phys. Rev. 172, 476 (1968).
[37]D. W. Taylor and P. Vashishta, Phys. Rev. B 5, 4410 (1972).
[38]G. Chanin, E. A. Lynton, and B. Serin, Phys. Rev. 114, 719 (1959).
[39]B. Mitrovic (unpublished).
[40]J. M. Daams and J. P. Carbotte, Can. J. Phys. 56, 1248 (1978).